DR. YIDA GAO (Orcid ID : 0000-0002-7409-9213)

Article type : Original Article

Dynamics of cell death across growth stages and the diel cycle in the dinoflagellate *Karenia Brevis*

Yida Gao[a,1] & Deana L. Erdner[a]

a Marine Science Institute, University of Texas at Austin, 750 Channelview Drive, Port Aransas, 78373, Texas, USA

1 Present address: Florida Fish and Wildlife Conservation Commission, Fish and Wildlife Research Institute, 100 8th Avenue SE, St. Petersburg, 33701, Florida, USA.

Correspondence

Y. Gao, Florida Fish and Wildlife Conservation Commission, Fish and Wildlife Research Institute, 100 8th Avenue SE, St. Petersburg, Florida 33701, USA

Telephone number: +1 512-870-7286; e-mail: yida.gao@utexas.edu

ABSTRACT

Recent evidence suggests that programmed cell death (PCD) can play a role in stress-induced decline and termination of harmful algal blooms. However, components of the PCD cascade, i.e. reactive oxygen species (ROS) and caspase-like activity, have also been observed in the absence of exogenous stress, where their activities and functions are unclear. Here we characterized the variability of prevalence of cell death, ROS and caspase-like activity at different growth phases and diel cycles in cultures of dinoflagellate *Karenia brevis*. Results show that ROS percentages increased with culture age and fluctuated in a phasing diel pattern, while caspase-like activity was observed throughout growth. In actively-growing *K. brevis* cells PCD components may be involved in key metabolic processes, while in stationary phase they may relate to stress acclimation. The circadian diel pattern of ROS may be explained by the balance between the metabolic generation of ROS and circadian rhythmicity of antioxidant enzymes. Overall, this work highlights not only the involvement of PCD components in the growth of marine phytoplankton, but the importance of understanding mechanisms controlling their accumulation, which would help to better interpret their presence in the field.

Keywords

Programmed cell death, reactive oxygen species, caspase-like activity, normal growth, diel variation

PREVIOUS studies have shown that programmed cell death (PCD), genetically-controlled forms of cell suicide, may play a role in decline and termination of phytoplankton blooms (Bidle 2016; Choi et al. 2017; Vardi et al. 1999). In algae, environmental stress can induce an increase of intracellular reactive oxygen species (ROS), which in turn elicits caspase-like enzyme activity (Cysteine dependent ASPartic acid proteASES) and leads to cell death (Bidle 2016; Gechev and Hille 2005). Therefore, ROS and caspase-like activity are considered to be an inducer and

executioner of PCD, respectively (Bidle 2016; Cohen 1998). The involvement of ROS and caspase-like activity in stress-induced cell death has been confirmed in many microalgal species (Segovia and Berges, 2009; Vardi et al. 1999; Zuppini et al. 2007), however, much less is known about their activities under replete culture conditions.

Understanding the variation of ROS and caspase-like activity under replete growth in phytoplankton can provide insights into their housekeeping functions and involvement in metabolic processes. While excessive accumulation of ROS can cause severe cellular damage (i.e. alteration of lipids, proteins and DNA) and cell death, lower levels of ROS are critical for redox signaling and the maintenance of cellular physiological functions (Schieber and Chandel 2014; Suzuki and Mittler 2006). In plants, ROS are generated from metabolic activities in chloroplasts, mitochondria and peroxisomes (Apel and Hirt 2004; Diaz and Plummer 2018), and their overall production is often higher during daytime as a result of photosynthesis (Foyer and Noctor 2005; Kim et al. 2004; Miller et al. 2010). This can be countered by stronger daytime activity of antioxidant enzymes that detoxify ROS, as has been reported in cultures of dinoflagellates (Okamoto and Colepicolo 2001; Okamoto et al. 2001) and green algae (Sigaud-Kutner et al. 2005). In phytoplankton populations, the dynamic balance between ROS production and scavenging processes would determine the prevalence of oxidative stress over a diel cycle; this pattern has not yet been examined in microalgae. On the time scale of culture growth, the capacity for ROS scavenging may decline with culture age, as indicated by down-regulation of gene expression for ROS detoxification enzymes at stationary phase in dinoflagellates (Johnson et al. 2012). Decreased scavenging may result in an increase in the prevalence of ROS as cultures age. The baseline level of caspase-like activity in phytoplankton populations may also vary across growth stages and even over the diel cycle, as recent research has implicated them in housekeeping roles such as cell proliferation, proteostasis (log-phase) and stress acclimation (stationary phase) in microorganisms (Algeciras-Schimnich et al. 2002; Bidle et al. 2010; Bouchard and Purdie 2011; Jauzein and Erdner 2013; Johnson et al. 2014; Johnson et al. 2012; Seth-Pasricha et al. 2019; Taroncher-Oldenburg et al. 1997; Thamatrakoln et al. 2012). Caspase-like activity, as a hallmark of PCD, has been observed in the field during dinoflagellate blooms (Vardi et al. 1999; Choi et al. 2017). Understanding the expression and non-death roles of this enzymatic activity across growth stages would help us better interpret their functions during a bloom event.

The objective of this research was to characterize the dynamics of cell death over both the course of culture growth and diel cycles in the toxic dinoflagellate *K. brevis*. In addition, we examined the prevalence of ROS and caspase-like activity to understand their functions under replete culture conditions. To determine changes across growth stages, replete *K. brevis* cultures were monitored for a 48-hour period during each of early-log, mid-log and stationary phase. In order to understand diel variation of these activities and their potential relationship to cell proliferation, another set of log-phase *K. brevis* cultures maintained under either 12:12 light:dark cycle (L:D) or continuous light were sampled every four hours for two consecutive days. Under each light environment, comparisons were made between expression of stress markers and cell cycle patterns. The involvement and non-death roles of ROS and caspase-like activity during each stages of phytoplankton growth are discussed, including potential mechanisms driving the diel cycle of ROS prevalence.

MATERIALS AND METHODS

Culture conditions and experimental setup

Growth stages. All experiments used xenic *K. brevis* clone SP3 cultured in L1 medium (Magaña and Villareal 2006). To prepare medium, seawater was filtered through 0.2 um polycap capsule filter (Whatman Inc., Maidstone, UK), adjusted to a salinity of 32 by the dilution of ultrapure water, and autoclaved prior to the addition of sterile L1 nutrient stocks (Guillard and Hargraves 1993). An inoculum culture was started (Day 0) at a cell density of 300 cells ml^{-1} in L1 medium and was maintained at 25 °C under cool white fluorescent light of ca. 90 μmol m^{-2} s^{-1} on a 12:12 L:D cycle.

Since unarmored *Karenia* are very delicate and sensitive to disturbance (Gentien et al. 2007; Lenes et al. 2013; Liu et al. 2002), the experimental setup was designed to reduce repeated sampling of the same flask. The inoculum culture was allowed to grow for four days, at which point 120 ml of culture was dispensed into each of ten 200 ml flasks. Three sets of triplicate flasks were designated as “early-log”, “mid-log” or “stationary”. These flasks were only sampled during the 48-hour monitoring period during their designated growth stage. The tenth flask was

established exclusively for monitoring growth. It was sampled periodically to determine cell density, as an indicator of when the experimental cultures reached the different growth stages. Specifically, cell densities of approximately 4,000 cells/ml, 9,000 cells/ml and 18,000 cells/ml in this flask indicated that the batch cultures were in early-log, mid-log and stationary stages, respectively. The cell densities corresponding to each growth stage were based on previous growth curves of SP3 cultures incubated under the same volume and conditions.

Sampling of the early-log, mid-log and stationary samples started on Day 9, Day 14 and Day 21, respectively. At each growth stage the first sample was taken at three hours after the beginning of light phase (time 0h) followed by subsequent sampling at 6h, 24h, 30h and 48h for measurement of cell density and percentages of cells staining for SYTOX, ROS and caspase-like activity.

Diel cycle. Duplicate, 2,000-ml inoculum cultures of strain SP3 were started at 500 cells/ml and grown under the same conditions as described under "Growth Stages" above, with the exception of light conditions: one was grown in 12:12 L:D, the other one was grown in continuous light. Before the experiment these two inoculum cultures had been continuously grown and transferred under 12:12 L:D for more than a year, which effectively synchronized their cell cycle to the light cycle (Vaulot 1995; Shi et al. 2013). When the cell concentration reached ~2,000 cells/ml, 50 ml of culture was dispensed into each of 36, 100-ml tissue flasks. Flasks were grouped into 12 sets of three, allowing triplicate flasks to be sacrificed at each sampling time. When cultures were in log phase under 12:12 L:D, the first sample was taken at two hours after the beginning of light phase (time 2h). Subsequent sampling occurred every four hours during two consecutive days. In continuous light, sampling started after cultures had been exposed to continuous light for seven days, and they were sampled at the same clock times as the ones in grown under 12:12 L:D. At every sampling point in both treatments, we measured cell density, percentages of cells with SYTOX, ROS and caspase-like activity, as well as the percentages of cells in each cell cycle phase.

Measurement of stress and cell death markers

SYTOX, ROS and caspase-like activity were measured using fluorescent stains as described below. All reagents produced green fluorescence, which was observed using an epifluorescent microscope (Olympus BX41, Tokyo, Japan) and a filter with a band pass excitation wavelength of 450–490 nm and long pass emission of 523 nm. Duplicate samples were collected from each culture vessel, and 50-100 cells were counted and examined in each sample using a Sedgewick Rafter chamber under epifluorescent microscope.

Cell death detection. Loss of cell membrane integrity, which is an indicator of cell death, was determined using SYTOX-green dye (S7020, Invitrogen, Carlsbad, CA). This reagent has a high affinity for double-stranded DNA and can only penetrate compromised plasma membranes. An aliquot of stock solution (5 mM in DMSO) was diluted into Phosphate-Buffered Saline (PBS) to prepare a 100-µM working solution. A 2.5-µl aliquot of the working solution was then added directly to a 500-µl sample of algal culture, making the final concentration of SYTOX-green dye 0.5 µM. Observations of SYTOX-stained cells were conducted after 40 min of dark incubation at room temperature. SYTOX percentages were calculated as: the number of cells with green fluorescence/ the number of intact cells.

ROS production. Intracellular ROS was detected using carboxy-H_2DCFDA (C400, Invitrogen). A stock solution of 10 mM carboxy-H_2DCFDA in DMSO was diluted with PBS to prepare a 100-µM working solution. The working solution was then mixed with algal sample at a 1:9 ratio, for a 10-µM final concentration of carboxy-H_2DCFDA. Green fluorescence generated by the oxidation of carboxy-H_2DCFDA was examined after 20 min dark incubation at room temperature. Percentages of cells with ROS were calculated as: the number of cells with green fluorescence/ total cell number.

Activity of caspase-like enzymes. A distinctive feature of PCD is the activation of caspase-like enzyme activity. Caspase-like activity was detected with Image-iT LIVE Green Poly Caspases Detection Kit (I35104, Invitrogen), which is based on a fluorescent inhibitor of caspases (FLICA). This FLICA reagent is able to detect activities of most caspases including caspase-1, -3, -4, -5, -6, -7, -8, and -9. For each experimental flask, 2 ml of culture were harvested, in replicate, by centrifugation at 500 g for 5 min, resuspended in 1X FLICA working reagent, and incubated for 60 min at room temperature in darkness. The FLICA reagent was then removed by

centrifugation (500 g, 5 min), and cells were resuspended in wash buffer before being observed on the epifluorescence microscope. Percentage of cells with caspase-like activity was calculated as: the number of cells with green fluorescence/ total cell number.

Live Cell Density

The densities of total morphologically intact cells were determined in duplicate from each culture vessel by counting under the microscope using a Sedgewick Rafter chamber after preservation with Lugol's iodine solution. Because light microscope counts include all morphologically distinguishable cells, densities of live cells from each flask were calculated as: averaged total morphologically intact cells per ml × (1 - averaged SYTOX proportion).

Flow cytometric cell cycle analysis

A 30-ml sample from each culture flask was harvested by centrifugation (500g, 5 min), and the resultant pellets were fixed in 2% glutaraldehyde and stored at 4 °C for at least 12 h. Fixed samples were centrifuged (500g, 5 min) to pellet the cells, and then resuspended in 1-mL ice cold absolute methanol and stored at -20 °C to extract cellular pigments. This step was used to reduce the interference between pigment autofluorescence and DNA stain fluorescence. Before flow cytometry analysis, samples were pelleted by centrifugation (500g, 5 min). Their DNA was stained by addition of 500 µl of 10 ug/mL propidium iodide (PI) in PBS containing 10 mg/ml RNase and 0.5% Tween 20 and incubation for at least 12 h at 4 °C. DNA analysis of the PI-stained cells was conducted on an Accuri C6 flow cytometer with 488 nm excitation (BD Biosciences, Franklin Lakes, NJ). Fluorescence of the DNA-bound PI stain was detected at 585 nm with "FL2 90% attenuation filter" (653175, BD Biosciences), and data were collected with 2-min fast inflow for each sample. Based on the flow cytometric data, the percentages of cells in each stage (G1, S, and G2+M) of the cell cycle were calculated using Flowjo 7.6 software. Since cells in the G2 or M phase have similar DNA content, flow cytometric analysis cannot distinguish these two phases; therefore, the two phases are categorized as G2+M.

Statistical analysis

In the "growth stages" experiment one-way repeated measures ANOVA (RM-ANOVA) was used to evaluate differences of PCD markers' prevalence among different growth stages. In the "diel cycle" experiment two-way RM-ANOVA was used to compare these parameters measured from different light cycle treatments in light/night hours. Tukey post-hoc test was performed for multiple comparisons. The α was set to 0.05. All statistical analyses were performed using SigmaPlot 14.

RESULTS

Stress and Death Marker Prevalence over Culture Growth

Sampling was conducted for 48 hours beginning on Day 9 (early-log phase), Day 14 (mid-log phase) and Day 21 (stationary phase) when cell densities in the "indicator" flask were around 4,000, 9,000 and 18,000 cells/ml, respectively (Fig. 1). The percentages of SYTOX positive cells were very low--less than 2% on average across all the growth stages, and live cell densities increased over time (Fig. 2A). The average ROS prevalence increased significantly ($p < 0.001$) from less than 10% in early-log phase (8.87 ± 3.64%) to approximately 50% of cells in mid-log (48.93 ± 7.55%) and stationary phases (52.67 ± 14.89%; Fig. 2B). In contrast, the average proportions of cells expressing caspase-like activity fluctuated strongly during culture growth (Fig. 2B; $p < 0.05$), ranging from a low of 23.89 ± 8.40% in mid-log phase to 55.72 ± 9.78% in stationary phase.

Stress and Death Marker Prevalence over Diel cycles

Cell densities, prevalence of stress/death markers, and cell cycle stages were determined every four hours during two diel cycles under 12:12 L:D and continuous light. Under both light conditions, total cell densities increased gradually over the two-day monitoring period (Fig. 3) and the percentages of SYTOX positive cells never exceeded 10% (data not shown). ROS proportions showed the same pattern under both 12:12 L:D and continuous light, with peak

prevalence during dark phase/circadian night hours and the lowest values during the light phase/circadian daytime hours (Fig. 4). With this pattern the prevalence of ROS during dark phase/circadian night hours was significantly higher than the light phase/circadian daytime hours ($p < 0.001$). However, the daily amplitude of ROS variation under 12:12 L:D was higher than under continuous light, mainly because the circadian daytime ROS prevalence in continuous light were stronger than the ones in the light phase of 12:12 L:D ($p < 0.001$). In contrast, the prevalence of caspase-like activity did not correlate with the light:dark cycle or circadian timing over the two diel cycles (Fig. 5). The proportion of cells showing caspase-like activity ranged from 3.20 ± 1.52% to 32.57 ± 3.02% (average 18.70 ± 4.57%) under 12:12 light cycle and from 10.83 ± 7.56 to 45.44 ± 4.44% (average 28.12 ± 4.92%) under continuous light.

Cell cycle stages varied according to the L:D cycle, and this synchronization was lost under continuous light. At the beginning of both light phases under 12:12 L:D, more than 85% of cells were in G1 phase (Fig. 6A: time 2h, time 26h). The proportion of cells undergoing DNA synthesis (S phase) was highest during the light phase, peaking at around 10 h into light (time 10h, time 34h). Peaks in the proportion of S phase cells corresponded to minima in the proportion of cells in G1. No consistent diel pattern was observed for G2+M phase during the two-day experiment. After being exposed to continuous light for seven days, the diel patterns for all cell cycle phases were reversed or lost (Fig. 6B). On the first day, the proportion of cells in G1 and S phase were highest at the beginning of the "circadian day" and "circadian night" respectively, which were opposite the patterns observed under 12:12 L:D. For the second day, there was little to no variation for any of the cell cycle stages, exhibiting a loss of synchronization of the cell cycle.

DISCUSSION

This study investigated how baseline cell death, ROS, and caspase-like activity change with growth, both at the short-term (diel) scale and the long-term (growth cycle) scale. In untreated cells, ROS percentages increased with culture age, and caspase-like activity was observed throughout growth. Neither of these two markers of the PCD cascade correlated with cell death. Observations of untreated cells over diel cycles suggested that while light may play an important

role in determining cell cycle patterns in *K. brevis*, neither light cycles nor cell cycles were correlated with diel variations of ROS and caspase-like activity.

Growth stages

Untreated cells showed evidence of ROS generation and caspase-like activity which varied along the growth curve but were not associated with cell death. This supports roles for both ROS and caspase-like activity in cellular metabolism and housekeeping functions. ROS prevalence in untreated *K. brevis* cultures was low in early-log phase and increased with culture age. On average about half of the cells in mid-log and stationary cultures had detectable ROS, although the underlying causes may be different. The observation of extensive ROS prevalence in mid-log phase may be a consequence of enhanced cellular metabolic processes. Significant production of ROS in exponential growth phase has been observed in the dinoflagellate *Margalefidinium polykrikoides* (Kim et al. 1999) and some raphidophyte species including *Heterosigma akashiwo* (Portune et al. 2010; Twiner and Trick 2000), *Chattonella antiqua* (Kim et al. 2004) and *C. marina* (Kawano et al. 1996; Liu et al. 2007; Oda et al. 1995). However, our result is the first report of high ROS prevalence during log phase in *K. brevis*. The ROS observed during rapid exponential growth has been attributed to increased mitochondrial or chloroplastic activity depending on the specific species (Kim et al. 2004; Portune et al. 2010; Twiner and Trick 2000). The observed high levels of ROS prevalence in stationary phase agrees with the results of Johnson et al. (2014), who observed ROS staining in more than 65% of stationary phase *K. brevis* cells. The transition from active growth to stationary phase represents a tremendous change of metabolic and physiological status. In *K. brevis*, this change is reflected in a major restructuring of the transcriptome for stress responses including repression of ROS detoxification/antioxidant pathways that may weaken ROS scavenging (Johnson et al. 2012). In addition, nutrient starvation in stationary phase may inhibit photosynthetic capacity leading to increased algal ROS generation, as has been observed in iron limited diatoms (Thamatrakoln et al. 2012).

Caspase-like activity was detected in more than 20% of cells in all the stages of growth. Bouchard and Purdie (2011) and Johnson et al. (2014) examined temporal variation in rates of

protein-normalized caspase-like activity in whole-cell lysates of *K. brevis* under normal conditions. Both of these studies revealed baseline cleavage activity of caspase-like enzymes along the growth curve, with highest activity at stationary phase, a pattern that is similar to our results using caspase labeling of cells. Caspase activity has been associated with non-death functions in both multicellular and unicellular organisms. In metazoans, caspases are involved in processes including cellular survival, differentiation, and proliferation (Algeciras-Schimnich et al. 2002). Increasing evidence of housekeeping functions of caspase-like activity has emerged for unicellular organisms. A high basal level of caspase activity was observed in exponentially growing archaeal cells, where it is responsible for cellular proteolytic activities that prevent accumulation of damaged proteins during active growth (Seth-Pasricha et al. 2019). In the diatom *Thalassiosira pseudonana* a constitutive presence of caspase-specific activity is found in about 14% of cells during log phase in non-stressed cultures (Bidle and Bender, 2008; Thamatrakoln et al. 2012). In *K. brevis*, caspase-like activity was lowest during mid-log phase (~24% of cells), despite the high ROS prevalence we observed during this growth stage. Caspase-like activity may not be triggered by ROS production during rapid growth because cells have a variety of alternative mechanisms to counter oxidative stress. For example, the bloom-forming diatom *Skeletonema costatum* increases expression of multiple genes related to oxidative stress in conditions that are favorable for bloom formation (Ogura et al. 2018). While prevalence of caspase-like activity varied throughout growth in *K. brevis*, the constitutive presence of this proteolytic activity along with very low cell death supports a role in beneficial housekeeping and regulatory functions.

As algal cells approach quiescence, caspase-like activity may be involved in the cellular response to physiological stress. For example, genomic and biochemical analyses of *T. pseudonana* from stationary phase show higher caspase-specific activity and up-regulation of gene expression associated with some types of metacaspases (homologues of caspase), which are hypothesized to assist in photosynthetic stress expressed by decreased Fv/Fm (Bidle and Bender 2008; Thamatrakoln et al. 2012). This may also be the case for *K. brevis*, as our results show the highest prevalence of caspase-like activity in stationary phase. This increase occurs at the same time as major changes related to the transition to quiescence in *K. brevis*, including transcriptome restructuring (Johnson et al. 2012) and the appearance of cyst-like structures (Bouchard and Purdie 2011).

Diel cycle

The presence of stress markers in untreated cells and their possible association with physiological processes like cell proliferation led us to investigate these same markers under a controlled environment at a finer temporal growth scale, that of the diel cycle. This included cultures grown under 12:12 L:D and continuous light, in order to examine the relationships between light cycles, cell cycles, and diel expression of intracellular ROS and caspase-like protease activity. The prevalence of cell death was low (less than 10%) in diel samples, and less than the average ROS and caspase-like activity, which again supports a general housekeeping role for these PCD components.

ROS prevalence exhibited a diel phasing pattern that does not correlate with light cycle or cell cycle. To our knowledge, there are no reports of diel variation of ROS expression in dinoflagellates. In this study, the observed peak of cell division and ROS prevalence both occurred during night phase under 12:12 L:D in *K. brevis*, therefore we hypothesized that ROS diel variation may be connected with active cell division. However, under continuous light the rhythm of cell cycle phasing was lost which indicates a loss of concentrated time for cell division, whereas the peak of ROS prevalence at circadian night hours persisted. These results suggest that ROS prevalence appears to be under circadian control, and cell division does not drive the observed ROS diel rhythm in *K. brevis*.

The observed diel variation of ROS prevalence may be attributable to the circadian rhythm of antioxidant enzymes previously reported in dinoflagellates and other algae. In phytoplankton, ROS production primarily occurs in the chloroplasts (photosynthesis) and mitochondria (respiration; Diaz and Plummer 2018; Møller 2001), and the maximal production of ROS generally occurs during the light hours as a result of active photosynthesis (Foyer et al. 1994; Foyer and Noctor 2005). In order to deal with the oxidative stress resulting from photosynthesis, many microorganisms exhibit a diel cycle of antioxidants peaking at daytime (Bucciarelli et al. 2007; Dupont et al. 2004; Jensen et al. 2011; Levy et al. 2006; Mella-flores et al. 2012; Okamoto and Colepicolo 2001; Sigaud-Kutner et al. 2005). For example, in cyanobacteria gene expression associated with ROS detoxification (i.e. superoxide dismutase (SOD) and catalase) is

significantly upregulated during the light hours (Jensen et al. 2011; Mella-flores et al. 2012). However, studies have also implicated an endogenous circadian clock, rather than light environment, in controlling different antioxidants in microalgae. Okamoto & Colepicolo (2001) tracked the diel change of antioxidant Fe-SOD (the main ROS scavenger in chloroplasts) and Mn-SOD (the main ROS scavenger in mitochondria) activities and abundances in the dinoflagellate *Lingulodinium polyedra* under 12:12 L:D and continuous light. They observed a solid circadian rhythmicity that increased and peaked at circadian early day hours and then decreased to the lowest value during circadian dark phase. This circadian time-keeping behavior may be beneficial for phytoplankton to deal with predictable oxidative challenges from daily variation of light conditions. In our experiment the generation of ROS during dark hours under 12:12 L:D would mainly be from mitochondrial activity, while both photosynthesis and respiration are sources of ROS in circadian dark hours under continuous light. Therefore, ROS generated from these metabolic processes may be effectively removed by antioxidant enzymes like Mn-SOD and Fe-SOD during circadian light hours, while those ROS produced during circadian dark hours would accumulate in cells. Toepel et al. (2008) also suggested similar circadian regulation of oxidative stress in the cyanobacterium *Cyanothece sp.*, as the expression of genes encoding SOD and catalase remain low in circadian dark hours under continuous light. Peroxiredoxin, a family of antioxidant proteins that are involved in controlling intracellular redox levels, are also reported to exhibit a conserved circadian rhythm persisting for days under constant light in *Synechococcus* and archaeal cells (Edgar et al. 2012). Thus, the circadian rhythm of different antioxidants may drive the observed diel variation of ROS prevalence.

Light does control cell cycle patterns in *K. brevis*, as exposure to continuous light for seven days "erased" the cell cycle pattern shaped by growth under 12:12 L:D. Diel variation of the cell cycle has been well documented in *K. brevis* (Brunelle et al. 2007; Van Dolah and Leighfield 1999; Van Dolah et al. 2008). Van Dolah et al. (2008) cultured multiple *K. brevis* strains under 16:8 L:D and recorded cell cycle patterns which were generally similar to the patterns observed here (12:12 L:D) in terms of the relationship with light and dark phases. Brunelle et al. (2007) transferred *K. brevis* cultures from 16:8 L:D to continuous light and monitored cell cycle patterns for three consecutive days, finding that the cell cycle of *K. brevis* was under circadian control as the pattern behaved similarly as observed in 16:8 L:D. However, based on our results it seems exposure to continuous light for seven days is enough to significantly disrupt the previous cell

cycle pattern. A similar effect was reported from dinoflagellate *Prorocentrum donghaiense*, as the amplitude of each cell cycle phase generally tended to decrease after 22 hours under continuous light (Shi et al. 2013).

Caspase-like activity does not correlate with the cell cycle in *K. brevis*, as the caspase-like activity showed a random fluctuation under different light environments. In metazoans, caspases are believed to serve as one of the checkpoints to make sure only healthy cells can proceed and complete cell division (Algeciras-Schimnich et al. 2002). If caspase-like activity plays a role in quality control of cell cycle progression in *K. brevis*, coherent peaks would be expected under the cell cycle pattern in 12:12 L:D. However, diel expression of caspase-like activity in *K. brevis* could be easily obscured if this protease activity was involved in other housekeeping functions that are not correlated to the cell cycle.

CONCLUSION

In the evolutionary history of aquatic photoautotrophs, PCD-related genes have existed in genomes for about 3 Ga (Summons et al. 1999; Yoon et al. 2004). The components of the PCD cascade must have some physiological benefit to unicellular algae otherwise they would have been lost from genomes long ago. While little cell death was observed during our experiments, ROS percentages increased with culture age and fluctuated in a phasing diel pattern, while prevalence of caspase-like activity was observed throughout growth, supporting their roles in cellular metabolism and housekeeping functions. In actively-growing *K. brevis* cells ROS and caspase-like activity may be involved in key metabolic processes (i.e. photosynthesis and respiration) and protein cleavage, respectively. The circadian pattern of ROS prevalence over a diel cycle in mid-log cultures may be explained by the balance between the metabolic generation of ROS and circadian rhythmicity of antioxidant enzymes, which are beneficial for dealing with daily predictable oxidative challenges. In contrast, caspase-like activity showed a random fluctuation under different light environments, thus this protease activity may be involved in multiple housekeeping functions. ROS and caspase-like activity are also prominent when culture growth slows or ceases. Our research revealed the highest extent of ROS and caspase-like activity at stationary phase, when these stress markers may relate to the transcriptome

restructuring (Johnson et al. 2012) and transformation in morphology (Bouchard and Purdie 2011) associated with the transition to quiescence. Overall, this work highlights not only the involvement of ROS and caspase-like activity in the growth of marine phytoplankton, but also the importance of understanding mechanisms controlling their accumulation.

ACKNOWLEDGEMENTS

We thank Dr. Paul Zimba from Texas A&M University-Corpus Christi for providing research facilities to us after the shutdown of UT Marine Science Institute due to Hurricane Harvey. This work was supported by the funding of "Ecology and Oceanography of HABs" from National Oceanic and Atmospheric Administration Center [grant number NA18NOS4780168]. This is ECOHAB publication #1002.

LITERATURE CITED

Algeciras-Schimnich A., Barnhart B. C. & Peter M. E. 2002. Apoptosis-independent functions of killer caspases. *Curr. Opin. Cell Biol.*, 14:721–726.

Apel K. & Hirt H. 2004. Reactive oxygen species: Metabolism, Oxidative Stress, and Signal Transduction. *Annu. Rev. Plant Biol.*, 55:373–399.

Bidle K. A., Haramaty L., Baggett N., Nannen J. & Bidle K. D. 2010. Tantalizing evidence for caspase-like protein expression and activity in the cellular stress response of Archaea. *Environ. Microbiol.*, 12:1161–1172.

Bidle K. D. 2016. Programmed Cell Death in Unicellular Phytoplankton. *Curr. Biol.*, 26:R594–R607.

Bidle K. D. & Bender S. J. 2008. Iron Starvation and Culture Age Activate Metacaspases and Programmed Cell Death in the Marine Diatom *Thalassiosira pseudonana*. *Eukaryot. Cell*, 7:223–236.

Bouchard J. N. & Purdie D. A. 2011. Temporal variation of caspase 3-like protein activity in cultures of the harmful dinoflagellates *Karenia brevis* and *Karenia mikimotoi*. *J. Plankton Res.*, 33:961–972.

Brunelle S. A., Hazard E. S., Sotka E. E. & Dolah F. M. Van. 2007. Characterization of a dinoflagellate cryptochrome blue-light receptor with a possible role in circadian control of the cell cycle. *J. Phycol.*, 43:509–518.

Bucciarelli E., Sunda W. G., Belviso S. & Sarthou G. 2007. Effect of the diel cycle on production of dimethylsulfoniopropionate in batch cultures of *Emiliania huxleyi*. *Aquat. Microb. Ecol.*, 48:73–81.

Choi C. J., Brosnahan M. L., Sehein T. R., Anderson D. M. & Erdner D. L. 2017. Insights into the loss factors of phytoplankton blooms: The role of cell mortality in the decline of two inshore Alexandrium blooms. *Limnol. Oceanogr.*, 62:1742–1753.

Cohen G. M. 1998. Role of caspases as the executioners of apoptosis. *Toxicol. Lett.*, 95:7.

Diaz J. M. & Plummer S. 2018. Production of extracellular reactive oxygen species by phytoplankton: past and future directions. *J. Plankton Res.*, 40:655–666.

Van Dolah F. M. & Leighfield T. A. 1999. Diel phasing of the cell-cycle in the Florida red tide dinoflagellate, *Gymnodinium breve*. *J. Phycol.*, 35:1404–1411.

Van Dolah F. M., Leighfield T. A., Kamykowski D. & Kirkpatrick G. J. 2008. Cell cycle behavior of laboratory and field populations of the Florida red tide dinoflagellate, *Karenia brevis*. *Cont. Shelf Res.*, 28:11–23.

Dupont C. L., Goepfert T. J., Lo P., Wei L. & Ahner B. A. 2004. Diurnal cycling of glutathione in marine phytoplankton: Field and culture studies. *Limnol. Oceanogr.*, 49:991–996.

Edgar R. S., Green E. W., Zhao Y., van Ooijen G., Olmedo M., Qin X., Xu Y., Pan M., Valekunja U. K., Feeney K. A., Maywood E. S., Hastings M. H., Baliga N. S., Merrow M., Millar A. J., Johnson C. H., Kyriacou C. P., O'Neill J. S. & Reddy A. B. 2012. Peroxiredoxins are conserved markers of circadian rhythms. *Nature*, 485:459–464.

Foyer C. H., Lelandais M. & Kunert K. J. 1994. Photooxidative stress in plants. *Physiol. Plant.*, 92:696–717.

Foyer C. H. & Noctor G. 2005. Redox Homeostasis and Antioxidant Signaling: A Metabolic Interface between Stress Perception and Physiological Responses. *Plant Cell*, 17:1866–1875.

Gechev T. S. & Hille J. 2005. Hydrogen peroxide as a signal controlling plant programmed cell death. *J. Cell Biol.*, 168:17–20.

Gentien P., Lunven M., Lazure P., Youenou A. & Crassous M. . 2007. Motility and autotoxicity in *Karenia mikimotoi* (Dinophyceae). *Philos. Trans. R. Soc. B Biol. Sci.*, 362:1937–1946.

Guillard R. R. L. & Hargraves P. E. 1993. Stichochrysis immobilis is a diatom, not a chrysophyte. *Phycologia*, 32:234–236.

Jauzein C. & Erdner D. L. 2013. Stress-related Responses in *Alexandrium tamarense* Cells Exposed to Environmental Changes. *J. Eukaryot. Microbiol.*, 60:526–538.

Jensen S. I., Steunou A., Bhaya D., Kühl M. & Grossman A. R. 2011. In situ dynamics of O2, pH and cyanobacterial transcripts associated with CCM, photosynthesis and detoxification of ROS. *ISME J.*, 5:317–328.

Johnson J. G., Janech M. G. & Van Dolah F. M. 2014. Caspase-like activity during aging and cell death in the toxic dinoflagellate *Karenia brevis*. *Harmful Algae*, 31:41–53.

Johnson J. G., Morey J. S., Neely M. G., Ryan J. C. & Van Dolah F. M. 2012. Transcriptome remodeling associated with chronological aging in the dinoflagellate, Karenia brevis. *Mar. Genomics*, 5:15–25.

Kawano I., Oda T., Ishimatsu A. & Muramatsu T. 1996. Inhibitory effect of the iron chelator desferrioxamine (Desferal) on the generation of activated oxygen species by *Chattonella marina*. *Mar. Biol.*, 126:765–771.

Kim C. S., Lee S. G., Kyu L. C., Kim H. G. & Jung J. 1999. Reactive oxygen species as causative agents in the ichthyotoxicity of the red tide dinoflagellate *Cochlodinium polykrikoides*. *J. Plankton Res.*, 21:2105–2115.

Kim D., Watanabe M., Nakayasu Y. & Kohata K. 2004. Production of superoxide anion and hydrogen peroxide associated with cell growth of *Chattonella antiqua*. *Aquat. Microb. Ecol.*, 35:57–64.

Lenes J., Walsh J. & Darrow B. 2013. Simulating cell death in the termination of *Karenia brevis* blooms: implications for predicting aerosol toxicity vectors to humans. *Mar. Ecol. Prog. Ser.*, 493:71–81.

Levy O., Achituv Y., Yacobi Y. Z., Dubinsky Z. & Stambler N. 2006. Diel ' tuning ' of coral metabolism : physiological responses to light cues. :273–283.

Liu G., Janowitz G. & Kamykowski D. 2002. Influence of current shear on *Gymnodinium breve* (Dinophyceae) population dynamics: a numerical study. *Mar. Ecol. Prog. Ser.*, 231:47–66.

Liu W., Au D. W. T., Anderson D. M., Lam P. K. S. & Wu R. S. S. 2007. Effects of nutrients, salinity, pH and light:dark cycle on the production of reactive oxygen species in the alga *Chattonella marina*. *J. Exp. Mar. Bio. Ecol.*, 346:76–86.

Magaña H. A. & Villareal T. A. 2006. The effect of environmental factors on the growth rate of *Karenia brevis* (Davis) G. Hansen and Moestrup. *Harmful Algae*, 5:192–198.

Mella-Flores D., Six C., Ratin M., Partensky F., Boutte C., Le Corguillé G., Marie D., Blot N., Gourvil P., Kolowrat C. & Garczarek L. 2012. *Prochlorococcus* and *Synechococcus* have Evolved Different Adaptive Mechanisms to Cope with Light and UV Stress. *Front. Microbiol.*, 3:1–20.

Miller G., Suzuki N., Ciftci-Yilmaz S. & Mittler R. 2010. Reactive oxygen species homeostasis and signalling during drought and salinity stresses. *Plant. Cell Environ.*, 33:453–467.

Møller I. M. 2001. Plant Mitochondria and oxidative stress: Electron Transport, NADPH Turnover, and Metabolism of Reactive Oxygen Species. *Annu. Rev. Plant Physiol. Plant Mol. Biol.*, 52:561–591.

Oda T., Moritomi J., Kawano I., Hamaguchi S., Ishimatsu A. & Muramatsu T. 1995. Catalase- and Superoxide Dismutase-induced Morphological Changes and Growth Inhibition in the Red Tide Phytoplankton *Chattonella marina*. *Biosci. Biotechnol. Biochem.*, 59:2044–2048.

Ogura A., Akizuki Y., Imoda H., Mineta K., Gojobori T. & Nagai S. 2018. Comparative genome and transcriptome analysis of diatom, Skeletonema costatum, reveals evolution of genes for harmful algal bloom. *BMC Genomics*, 19:1–12.

Okamoto O. K. & Colepicolo P. 2001. Circadian Protection against Reactive Oxygen Species Involves Changes in Daily Levels of the Manganese- and Iron-Containing Superoxide Dismutase Isoforms in Lingulodinium polyedrum. *Biol. Rhythm Res.*, 32:439–448.

Okamoto O. K., Robertson D. L., Fagan T. F., Hastings J. W. & Colepicolo P. 2001. Different Regulatory Mechanisms Modulate the Expression of a Dinoflagellate Iron-Superoxide Dismutase. *J. Biol. Chem.*, 276:19989–19993.

Portune K. J., Craig Cary S. & Warner M. E. 2010. Antioxidant enzyme response and reactive oxygen species production in marine Raphidophytes. *J. Phycol.*, 46:1161–1171.

Schieber M. & Chandel N. S. 2014. ROS Function in Redox Signaling and Oxidative Stress. *Curr. Biol.*, 24:R453–R462.

Segovia M. & Berges J. A. 2009. Inhibition of caspase-like activities prevents the appearance of reactive oxygen species and dark-induced apoptosis in the unicellular chlorophyte *dunaliella tertiolecta*. *J. Phycol.*, 45:1116–1126.

Seth-Pasricha M., Senn S., Sanman L. E., Bogyo M., Nanda V., Bidle K. A. & Bidle K. D. 2019. Catalytic linkage between caspase activity and proteostasis in Archaea. *Environ. Microbiol.*, 21:286–298.

Shi X., Zhang H. & Lin S. 2013. Tandem Repeats, High Copy Number and Remarkable Diel Expression Rhythm of Form II RuBisCO in *Prorocentrum donghaiense* (Dinophyceae).Yamazaki S. (ed.). *PLoS One*, 8:e71232.

Sigaud-Kutner T. C. S., Neto A. M. P., Pinto E. & Colepicolo P. 2005. Diel activities of antioxidant enzymes, photosynthetic pigments and malondialdehyde content in stationary-phase cells of Tetraselmis gracilis (Prasinophyceae). *Aquat. Bot.*, 82:239–249.

Summons R. E., Jahnke L. L., Hope J. M. & Logan G. A. 1999. 2-Methylhopanoids as biomarkers for cyanobacterial oxygenic photosynthesis. *Nature*, 400:554–557.

Suzuki N. & Mittler R. 2006. Reactive oxygen species and temperature stresses: A delicate balance between signaling and destruction. *Physiol. Plant.*, 126:45–51.

Taroncher-Oldenburg G., Kulis D. M. & Anderson D. M. 1997. Toxin variability during the cell cycle of the dinoflagellate *Alexandrium fundyense*. *Limnol. Oceanogr.*, 42:1178–1188.

Thamatrakoln K., Korenovska O., Niheu A. K. & Bidle K. D. 2012. Whole-genome expression analysis reveals a role for death-related genes in stress acclimation of the diatom *Thalassiosira pseudonana*. *Environ. Microbiol.*, 14:67–81.

Toepel J., Welsh E., Summerfield T. C., Pakrasi H. B. & Sherman L. A. 2008. Differential Transcriptional Analysis of the Cyanobacterium *Cyanothece sp.* Strain ATCC 51142 during Light-Dark and Continuous-Light Growth. *J. Bacteriol.*, 190:3904–3913.

Twiner M. J. 2000. Possible physiological mechanisms for production of hydrogen peroxide by the ichthyotoxic flagellate *Heterosigma akashiwo*. *J. Plankton Res.*, 22:1961–1975.

Vardi A., Berman-Frank I., Rozenberg T., Hadas O., Kaplan A. & Levine A. 1999. Programmed cell death of the dinoflagellate *Peridinium gatunense* is mediated by CO2 limitation and oxidative stress. *Curr. Biol.*, 9:1061–1064.

Vaulot D. 1995. The Cell Cycle of Phytoplankton: Coupling Cell Growth to Population Growth. *In*: Molecular Ecology of Aquatic Microbes. Berlin, Heidelberg, Springer Berlin Heidelberg. p. 303–322.

Yoon H. S., Hackett J. D., Ciniglia C., Pinto G. & Bhattacharya D. 2004. A Molecular Timeline for the Origin of Photosynthetic Eukaryotes. *Mol. Biol. Evol.*, 21:809–818.

Zuppini A., Andreoli C. & Baldan B. 2007. Heat Stress: an Inducer of Programmed Cell Death in *Chlorella saccharophila*. *Plant Cell Physiol.*, 48:1000–1009.

FIGURE LEGEND

Figure 1: Change in cell densities of *Karenia brevis* cells in the "indicator" flask over time. Black arrows indicate the day when the experiment started for early-log phase (Day 9), mid-log phase (Day 14) and stationary phase (Day 21). Data points show average values obtained from duplicate measurements, and error bars show standard deviation.

Figure 2: Cellular stress responses under controlled environment in *Karenia brevis* cells at early log phase, mid-log phase and stationary phase. (A) Average proportions of cells stained with SYTOX and live cell densities during the 48-hour sample period at early-log, mid-log and stationary phases. (B) Average proportions of cells showing reactive oxygen species and caspase-like activity during the 48-hour sample period at early-log, mid-log and stationary phases. Error bars show standard deviation of the replicates (n = 30).

Figure 3: Total cell densities under 12:12 light cycle (open triangles, dashed line) and continuous light (filled circles, solid line). Data points show average values obtained from triplicate cultures, and error bars show standard deviation of the replicates (n = 3). Shaded areas show the dark phase for 12:12 L:D, and circadian dark hours under continuous light.

Figure 4: Proportion of cells showing ROS labeling during two diel cycles under 12:12 light (open triangles, dashed line) and continuous light (filled circles, solid line). Data points show average values obtained from triplicate cultures, and error bars show standard deviation of the replicates (n = 3). Shaded areas show dark phase for 12:12 L:D, and circadian dark hours under continuous light.

Figure 5: Proportion of cells showing caspase-like activity during two diel cycle under 12:12 L:D (open triangles, dashed line) and continuous light (filled circles, solid line). Data points show average values obtained from triplicate cultures, and error bars show standard deviation of the replicates (n = 3). Shaded areas show dark phase for 12:12 L:D, and circadian dark hours under continuous light.

Figure 6: Percentages of cells in each cell cycle phase during two diel cycles under 12:12 L:D (A) and continuous light (B). Data points show average values obtained from triplicate cultures, and error bars show standard deviation of the replicates (n = 3). Shaded areas indicate dark period of 12:12 L:D, and bold black rectangles indicate circadian dark hours under continuous light.

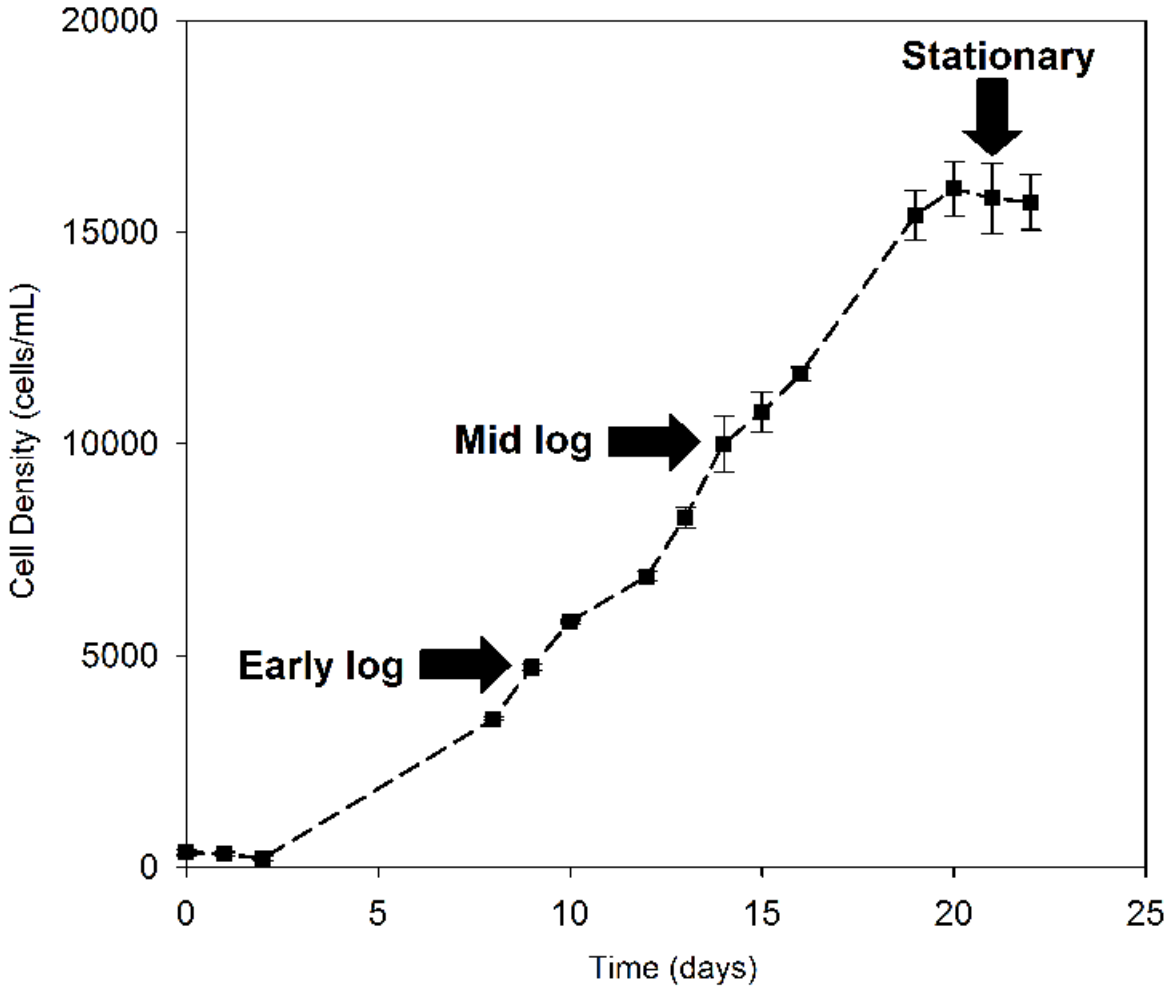

jeu_12874_f2.pdf

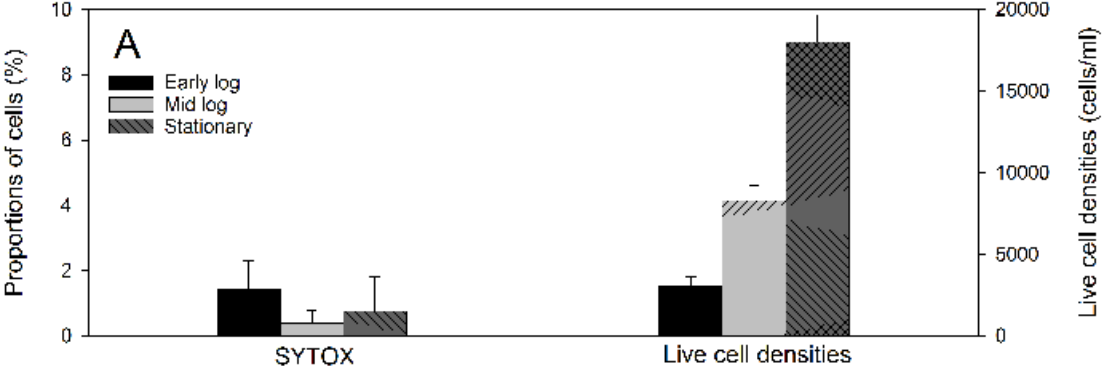

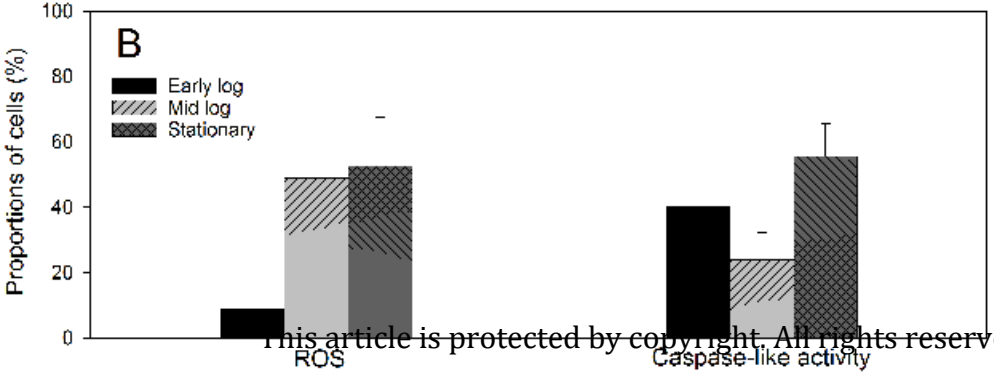

jeu_12874_f3.pdf

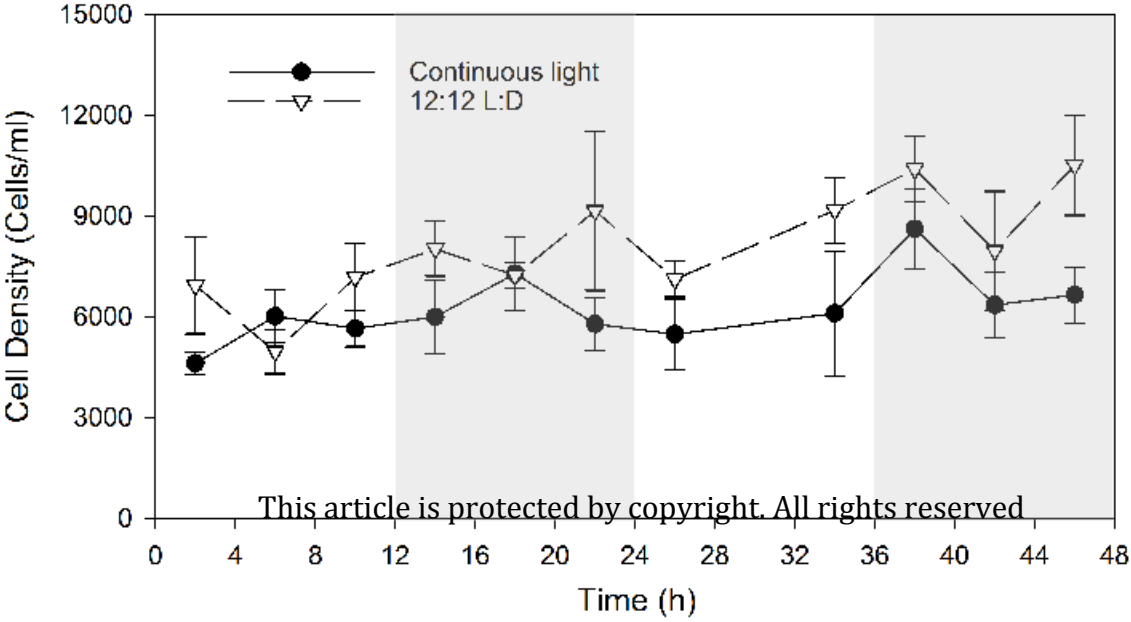

jeu_12874_f4.pdf

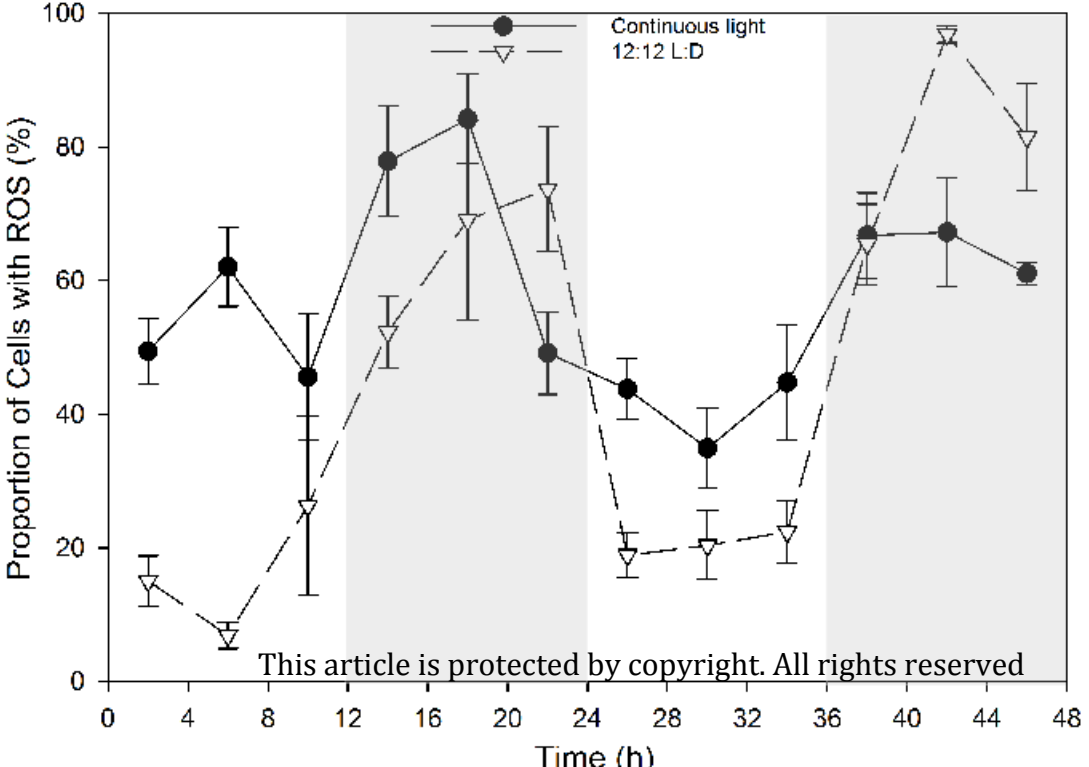

jeu_12874_f5.pdf